nature neuroscience

Parvalbumin interneurons mediate neuronal circuitry–neurogenesis coupling in the adult hippocampus

Juan Song[1–3], Jiaqi Sun[1,4,8], Jonathan Moss[5,8], Zhexing Wen[1,2,8], Gerald J Sun[1,6], Derek Hsu[1], Chun Zhong[1,2], Heydar Davoudi[1,7], Kimberly M Christian[1,2], Nicolas Toni[5,9], Guo-li Ming[1,2,6,9] & Hongjun Song[1,2,6,9]

Using immunohistology, electron microscopy, electrophysiology and optogenetics, we found that proliferating adult mouse hippocampal neural precursors received immature GABAergic synaptic inputs from parvalbumin-expressing interneurons. Recently shown to suppress adult quiescent neural stem cell activation, parvalbumin interneuron activation promoted newborn neuronal progeny survival and development. Our results suggest a niche mechanism involving parvalbumin interneurons that couples local circuit activity to the diametric regulation of two critical early phases of adult hippocampal neurogenesis.

One fundamental question in stem cell biology is whether and how niche factors couple tissue demands to the production of proper numbers of progeny from somatic stem cells. In the adult subgranular zone (SGZ), a substantial loss of newborn progeny occurs during the first 4 d after they are born[1–4]. Adult hippocampal neurogenesis occurs in a dynamic neuronal network; thus, we hypothesized that the local circuit activity may serve as an effective indicator of current tissue demands and provide a signal to regulate this critical event.

We used retroviruses expressing GFP to birth-date proliferating neural progenitors in the adult mouse SGZ[5]. At 4 d post viral injection (dpi), 92% of GFP$^+$ cells were minichromosome maintenance complex component 2 (MCM2)$^+$ and 81% were doublecortin (DCX)$^+$ MCM2$^+$ proliferating neuroblasts (**Supplementary Fig. 1**). Whole-cell recordings in acute slices showed that 95% of the GFP$^+$ cells that we recorded responded to GABA ($n = 37$; **Supplementary Fig. 2a**). Confocal imaging analysis revealed a close association of GFP$^+$ cells with synapsin$^+$ glutamate decarboxylase 1 (GAD67)$^+$ GABAergic presynaptic boutons (**Supplementary Fig. 2b** and **Supplementary Movie 1**). As previously shown[6,7], presynaptic terminals onto GFP$^+$ newborn progeny were observed by immuno-electron microscopy (**Supplementary Fig. 2c**). Although none of the GFP$^+$ cells that we recorded ($n = 55$) exhibited any spontaneous or evoked postsynaptic currents (PSCs) in response to 0.1-Hz field stimulation (**Supplementary Fig. 2d**), we recorded bicuculline-sensitive PSCs in 14.3% of GFP$^+$ cells following 5-Hz stimulation ($n = 35$; **Supplementary Fig. 2e**), suggesting that these synapses may be immature. This result contrasts with what is observed in the adult subventricular zone, where neuroblasts are activated by tonic GABA with no apparent synapses[8].

We next explored sources of GABAergic inputs. Confocal and light microscopy analyses revealed close associations of parvalbumin (PV)-expressing synapsin$^+$ puncta with GFP$^+$ cells at 4 dpi (**Supplementary Fig. 3a** and **Supplementary Movie 2**), including GFP$^+$ cells that were proliferating (MCM2$^+$; **Supplementary Fig. 3b**). Immuno-electron microscopy revealed symmetric synaptic contacts between vesicle-filled PV$^+$ axonal terminals and newborn progeny (**Fig. 1a**,**b** and **Supplementary Fig. 4a**–**f**), which were similar to those between PV$^+$ neurons and GFP$^-$ mature neurons (**Fig. 1c** and **Supplementary Fig. 4m**–**p**). Notably, we found various relationships between PV$^+$ axons and newborn progeny, ranging from proximal PV$^+$ boutons to mature-looking symmetric synapses (**Supplementary Fig. 4a**–**l**).

To determine whether observed synaptic structures are functional, we selectively expressed channelrhodopsin-2 (ChR2)–yellow fluorescent protein (YFP) in dentate PV$^+$ neurons using adult *Pvalb-cre* mice[9] and labeled proliferating neural progenitors with red fluorescent protein (RFP; **Supplementary Fig. 5**). Light stimulation at 8 Hz, but not at 0.1 Hz, led to GABAergic PSCs in 17% of the RFP$^+$ cells that we examined at 4 dpi in acute slices ($n = 48$; **Fig. 1d**). The low induction rate, small amplitude and broad distribution of rise times of evoked PSCs recorded in RFP$^+$ cells reflect characteristics of immature synapses (**Fig. 1e**–**g**). Blockade of glutamatergic synaptic transmission had no effect on PSCs (**Fig. 1e**,**f**), supporting the presence of monosynaptic connections from PV$^+$ neurons. Notably, optogenetic activation of somatostatin (SST)-expressing interneurons evoked PSCs in mature dentate granule neurons, but not in RFP$^+$ cells (**Fig. 1e**).

The identification of PV$^+$ neurons as one source of synaptic inputs onto newborn progeny, although not eliminating the possibility of inputs from other neurons[7,10], provides an entry point to investigate how local circuitry may regulate these progeny *in vivo*. We labeled proliferating neural progenitors with a thymidine analog, ethynyl deoxyuridine (EdU), and then applied light-induced activation of ChR2$^+$ PV$^+$ interneurons between 1 and 4 dpi (**Supplementary Fig. 6a**). Consistent with previous findings[1–4], stereological quantification in the no-light sham group showed a significant decrease in the number of EdU$^+$ cells in the adult SGZ from 1 to 4 dpi ($P = 6.5 \times 10^{-7}$; **Fig. 2a**,**b**). Notably, 8-Hz light stimulation led to significant increases in the numbers of EdU$^+$ cells ($P = 5.8 \times 10^{-4}$) and EdU$^+$ DCX$^+$ neuronal progeny ($P = 1.8 \times 10^{-3}$) at 4 dpi compared with the sham no-light treatment (**Fig. 2**). The survival

[1]Institute for Cell Engineering, Johns Hopkins University School of Medicine, Baltimore, Maryland, USA. [2]Department of Neurology, Johns Hopkins University School of Medicine, Baltimore, Maryland, USA. [3]Department of Pharmacology and Neuroscience Center, University of North Carolina School of Medicine, Chapel Hill, North Carolina, USA. [4]School of Life Sciences, Tsinghua University, Beijing, China. [5]Department of Fundamental Neurosciences, University of Lausanne, Lausanne, Switzerland. [6]The Solomon H. Snyder Department of Neuroscience, Johns Hopkins University School of Medicine, Baltimore, Maryland, USA. [7]Department of Biomedical Engineering, Johns Hopkins University School of Medicine, Baltimore, Maryland, USA. [8]These authors contributed equally to this work. [9]These authors jointly directed this work. Correspondence should be addressed to H.S. (shongju1@jhmi.edu), N.T. (nicolas.toni@unil.ch) or G.M. (gming1@jhmi.edu).

Received 19 August; accepted 8 October; published online 10 November 2013; doi:10.1038/nn.3572

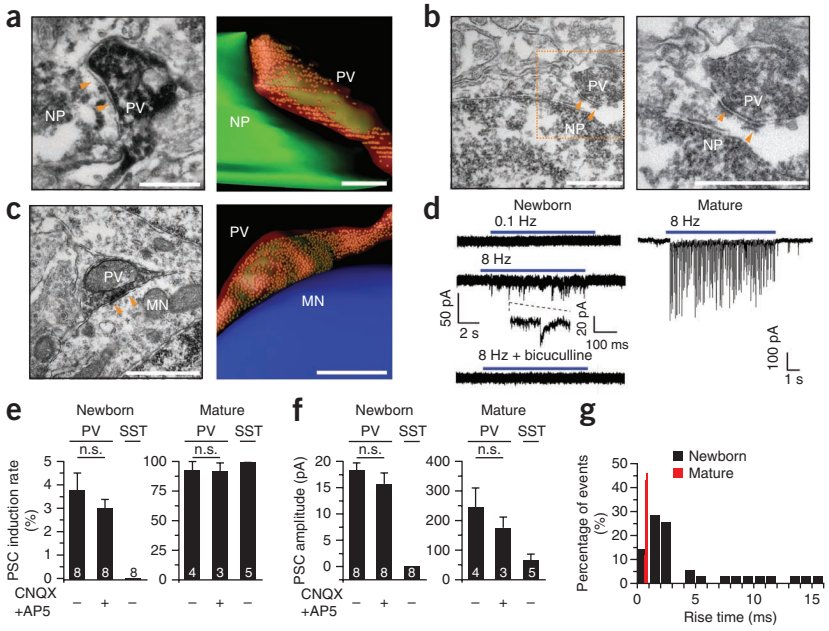

Figure 1 PV+ interneurons form immature synaptic inputs onto proliferating newborn progeny in the adult dentate gyrus. (**a**–**c**) Sample images and serial reconstructions of symmetrical synaptic contacts (arrowheads) between vesicle-filled PV+ axon terminals and newborn progeny (NP, **a**,**b**; scale bars, 0.5 µm) or unlabeled mature neurons (MN, **c**; scale bars, 1 µm) (**Supplementary Fig. 4**). (**d**) Sample traces of whole-cell voltage-clamp recording of a RFP+ new progeny and a mature granule cell in the same preparation following light stimulation (472 nm, 5 ms) of ChR2-expressing PV+ neurons. (**e**–**g**) Summaries of induction rate (**e**), mean amplitude (**f**) and distribution of rise times (**g**) of evoked PSCs recorded from RFP+ newborn progeny at 4 dpi and from mature granule neurons following 8-Hz light stimulation of ChR2-expressing PV+ or SST+ neurons. Numbers in bars indicate cell numbers. Means ± s.e.m. (n.s., $P > 0.1$, Student's t test) (**Supplementary Table 1**).

effect was accompanied by a reduction in dying cells, identified by pyknotic nuclei surrounded by Iba-1+ microglia (**Supplementary Fig. 6b**,**c**), as previously reported[1]. NeuroD has been suggested to promote newborn neuron survival during adult SGZ neurogenesis[11,12]. Indeed, there was a significant increase in the number of EdU+ NeuroD+ cells following light stimulation ($P = 0.014$; **Supplementary Fig. 7a**). In contrast, percentages of EdU+ cells that remained in cell cycle (MCM2+) or underwent neuronal differentiation (DCX+) were not different (**Supplementary Fig. 7b**,**c**). Notably, similar optogenetic manipulation of dentate SST+ interneurons had no effect (**Fig. 2** and **Supplementary Fig. 7b**,**c**).

To assess the role of endogenous PV+ neuron activity on newborn progeny survival, we selectively expressed the halorhodopsin NpHR in dentate PV+ neurons and optogenetically suppressed NpHR+ PV+ neurons between 1 and 4 dpi (**Supplementary Fig. 8a**–**c**). Stereological quantification revealed a further decrease in EdU+ MCM2+ proliferating neural precursors and DCX+ EdU+ neuronal progeny from 1 to 4 dpi following PV+ neuron suppression (**Fig. 3a**,**b**). The number of dying cells surrounded by Iba-1+ microglia increased (light, 1,244 ± 128 cells per mm^3; no light, 856 ± 102 cells per mm^3; $n = 3$ mice). No difference was found for cell cycle exit or neuronal differentiation of EdU+ cells (**Supplementary Fig. 8d**,**e**). An independent approach to suppress PV+ neuron activity using Arch showed similar effects as NpHR, whereas SST+ neuron suppression had no effect (**Fig. 3a**,**b** and **Supplementary Fig. 8d**,**e**). Notably, our optogenetic manipulations did not appear to affect general properties of mature dentate granule neurons (**Supplementary Fig. 9**).

Loss of proliferating precursors could have a bigger effect on the ultimate number of mature adult-born neurons than the loss of individual post-mitotic neurons (**Fig. 3c**). Indeed, PV+ neuron suppression between 1 and 4 dpi led to an 18.9% decrease in the number of EdU+ MCM2+ proliferating neural progeny at 4 dpi and a 49% decrease in the number of EdU+ NeuN+ neurons at 30 dpi ($n = 3$ mice).

Adult neurogenesis is dynamically regulated by external stimuli[13]. We introduced mice to an enriched environment between 1 and 4 dpi, an experience known to increase PV+ neuron activity[14]. This treatment substantially increased the numbers of EdU+, EdU+ DCX+ and EdU+ NeuroD+ progeny at 4 dpi compared with mice in standard conditions (**Fig. 3d**,**e** and **Supplementary Fig. 8h**). PV+ neuron suppression largely abolished the survival effect of an enriched environment (**Fig. 3e**). Thus, PV+ neuron activity is also involved in experience-dependent regulation of early critical phases of adult hippocampal neurogenesis.

Finally, we examined whether PV+ neuron activity continues to influence neuronal progeny beyond 4 dpi. Indeed, PV+ neuron–induced synaptic activation was detected at 7 dpi (**Supplementary Fig. 10a**). Optogenetic activation of PV+ neurons between 4 and 7 dpi promoted dendritic development of newborn neurons, whereas suppression of PV+ neuron activity had the opposite effect (**Supplementary Fig. 10b**–**f**).

Here we identified a previously unknown neuronal circuitry–based niche mechanism regulating proliferating neuronal progeny survival and their development via local PV+ interneuron activity. Although PV+ neurons make direct synaptic contacts with these newborn progeny, the optogenetic approach that we used does not rule out potential indirect contributions from circuitry modulation or factors other than GABA. In sharp contrast with the increased survival of newborn progeny, PV+ neuron activation, via nonsynaptic GABAergic signaling, inhibits adult quiescent neural stem cell activation[9]. Together, these results reveal a marked diametric regulation of two early critical steps of adult neurogenesis via PV+ neuron activity (**Supplementary Fig. 11a**).

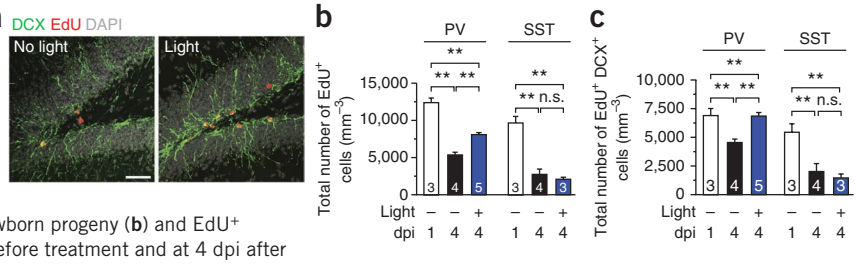

Figure 2 Activation of PV+, but not SST+, interneurons in the dentate gyrus promotes survival of proliferative newborn progeny during early phases of adult hippocampal neurogenesis. (**a**) Sample confocal images of staining of EdU, DCX and DAPI of the dentate gyrus after either the sham no-light treatment or 8-Hz light stimulation of ChR2+ PV+ neurons. Scale bar, 50 µm. (**b**,**c**) Summaries of stereological quantifications of total numbers of EdU+ newborn progeny (**b**) and EdU+ DCX+ newborn neuronal progeny (**c**) in the SGZ at 1 dpi before treatment and at 4 dpi after different treatments. Numbers in bars indicate number of mice used. Means ± s.e.m. (**$P < 0.01$; n.s., $P > 0.1$; one-way ANOVA; **Supplementary Table 1**).

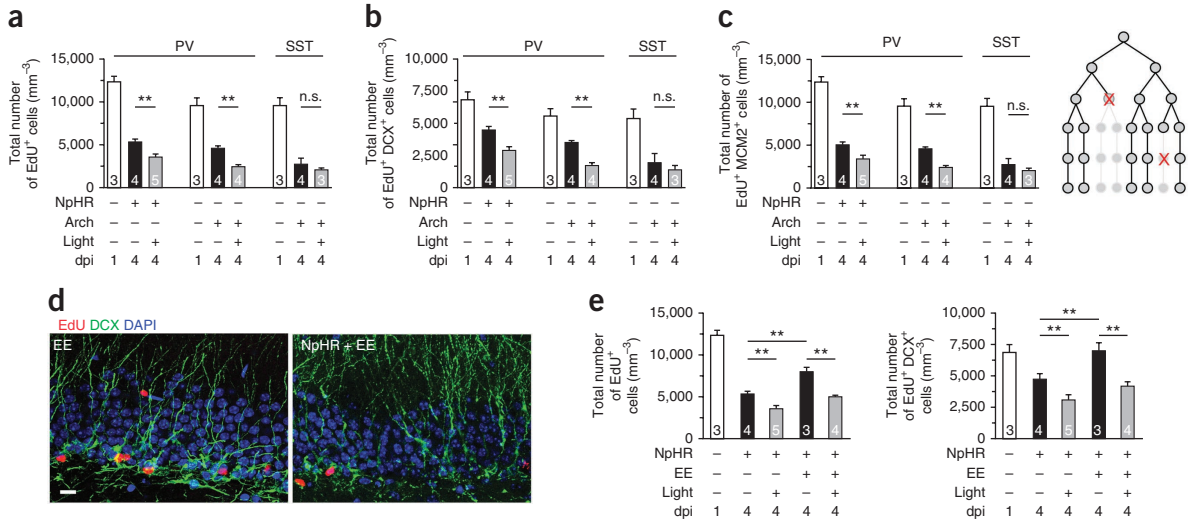

Figure 3 Suppression of PV+, but not SST+, interneuron activity in the adult dentate gyrus decreases survival of newborn progeny in the normal and enriched environment. (**a**,**b**) Data are presented as in **Figure 2b**,**c**. Numbers in bars indicate number of mice used. Means ± s.e.m. (**$P < 0.01$; n.s., $P > 0.1$; one-way ANOVA and Student's *t* test). (**c**) Left, stereological quantifications of total numbers of EdU+ cells that remained MCM+, indicative of active proliferation, at 1 and 4 dpi. Means ± s.e.m. (**$P < 0.01$; one-way ANOVA). Right, death of a proliferating progenitor leads to elimination of all its progeny, which potentially has a bigger effect on the final cell number than cell death of individual post-mitotic neurons. (**d**) Sample confocal images of staining for EdU, DCX and DAPI in the adult dentate gyrus at 4 dpi with light stimulation or sham treatment, in normal or enriched environments (EE), between 1 and 4 dpi. Scale bar, 10 μm. (**e**) Summaries of stereological quantifications, presented as in **a** and **b**. The same data under the normal condition from **a** and **b** are re-plotted for comparison. Means ± s.e.m. (**$P < 0.01$; two-way ANOVA and Student's *t* test; **Supplementary Table 1**).

Computational models have suggested advantages of circuit activity–neurogenesis coupling for temporal storage and memory clearing in the adult hippocampus[15,16]. Experimental evidence also suggests that a proper rate of both addition and elimination of new neurons optimizes behavioral outcomes in animal models[17,18]. What are the potential advantages of such a diametric mode of neuronal circuitry–neurogenesis coupling? First, it promotes an adaptive regulation of adult neurogenesis; a lack of dentate neuronal activity minimizes the need to retain and develop new neurons that have just been born, but increases the quiescent neural stem cell pool via symmetric cell division to prepare for the future. Second, it facilitates time-stamping of a specific cohort of newborn neurons during a period of heightened dentate activity by increasing their survival while simultaneously suppressing generation of new neurons from neural stem cell activation. This could be particularly important, as recent behavioral studies have suggested a critical contribution of newborn neurons at specific developmental stages to hippocampal function[13,19]. Our findings also point to the presence of multiple critical periods in regulating progeny survival via circuit-based, activity-dependent mechanisms[20] (**Supplementary Fig. 11b**), which may facilitate the development of new strategies to enhance functional repair from endogenous or transplanted neurons after injury and degenerative neurological disorders.

METHODS

Methods and any associated references are available in the online version of the paper.

Note: Any Supplementary Information and Source Data files are available in the online version of the paper.

ACKNOWLEDGMENTS

We thank members of the Song and Ming laboratories for discussion, L. Tsai and K. Deisseroth for initial help with optogenetics, and Q. Hussaini, Y. Cai and L. Liu for technical support. The electron microscopy images were acquired at the electron microscopy facility of the University of Lausanne. This work was supported by grants from the US National Institutes of Health (NS047344, ES021957) and The Brain & Behavior Research Foundation to H.S., from the US National Institutes of Health (NS048271, HD069184), the Dr. Miriam and Sheldon G. Adelson Medical Research Foundation, The Brain & Behavior Research Foundation and Maryland Stem Cell Research Fund to G.M., from the Swiss National Science Foundation (PP00A-119026/1) to N.T., from The Brain & Behavior Research Foundationand Maryland Stem Cell Research Fund to K.M.C., by postdoctoral fellowships from Maryland Stem Cell Research Fund to J. Song, Z.W. and C.Z., from the Fondation Leenaards to J.M., and by a pre-doctoral fellowship from The Children's Tumor Foundation to G.J.S.

AUTHOR CONTRIBUTIONS

J. Song led and contributed to all aspects of the study. J.M. and N.T. performed electron microscopy analyses. J. Sun, Z.W., G.J.S., D.H., C.Z., H.D. and K.M.C. contributed to tool development and data collection and analyses. G.M. and H.S. supervised the project and wrote the manuscript.

COMPETING FINANCIAL INTERESTS

The authors declare no competing financial interests.

1. Sierra, A. *et al. Cell Stem Cell* **7**, 483–495 (2010).
2. Snyder, J.S. *et al. J. Neurosci.* **29**, 14484–14495 (2009).
3. Kronenberg, G. *et al. J. Comp. Neurol.* **467**, 455–463 (2003).
4. Mandyam, C.D., Harburg, G.C. & Eisch, A.J. *Neuroscience* **146**, 108–122 (2007).
5. Ge, S. *et al. Nature* **439**, 589–593 (2006).
6. Kaplan, M.S. & Bell, D.H. *J. Neurosci.* **4**, 1429–1441 (1984).
7. Tozuka, Y., Fukuda, S., Namba, T., Seki, T. & Hisatsune, T. *Neuron* **47**, 803–815 (2005).
8. Liu, X., Wang, Q., Haydar, T.F. & Bordey, A. *Nat. Neurosci.* **8**, 1179–1187 (2005).
9. Song, J. *et al. Nature* **489**, 150–154 (2012).
10. Markwardt, S.J., Dieni, C.V., Wadiche, J.I. & Overstreet-Wadiche, L. *Nat. Neurosci.* **14**, 1407–1409 (2011).
11. Gao, Z. *et al. Nat. Neurosci.* **12**, 1090–1092 (2009).
12. Kuwabara, T. *et al. Nat. Neurosci.* **12**, 1097–1105 (2009).
13. Ming, G.L. & Song, H. *Neuron* **70**, 687–702 (2011).
14. Mann, E.O. & Paulsen, O. *Trends Neurosci.* **30**, 343–349 (2007).
15. Deisseroth, K. *et al. Neuron* **42**, 535–552 (2004).
16. Chambers, R.A., Potenza, M.N., Hoffman, R.E. & Miranker, W. *Neuropsychopharmacology* **29**, 747–758 (2004).
17. Kim, W.R. *et al. Eur. J. Neurosci.* **29**, 1408–1421 (2009).
18. Sahay, A. *et al. Nature* **472**, 466–470 (2011).
19. Gu, Y. *et al. Nat. Neurosci.* **15**, 1700–1706 (2013).
20. Tashiro, A., Sandler, V.M., Toni, N., Zhao, C. & Gage, F.H. *Nature* **442**, 929–933 (2006).

ONLINE METHODS

Construction, production and stereotaxic injection of engineered retroviruses and AAV. Engineered murine oncoretroviruses expressing GFP or RFP were used to birth-date and label proliferating cells and their progeny as previously described[5,21,22]. For experiments without optogenetic manipulations, adult mice (8 weeks old, female, C57BL/6 background; Charles River) housed under the standard condition or enriched environment[23] were anesthetized and retroviruses were stereotaxically injected into the dentate gyrus at two sites as previously described[5,22]. Immunohistological or electrophysiological analysis was performed at 2–10 dpi as previously described[5,22]. Cre-dependent recombinant AAV vectors were used for cell type–specific transgene expression[24–26]. AAV vectors were obtained from vector cores of University of Pennsylvania and University of North Carolina. Transgenic *Pvalb-cre* (B6;129P2-*Pvalb*$^{tm1(cre)Arbr}$/J) and *Sst-cre* (mixed background, *Sst*$^{tm2.1(cre)Zjh}$/J) mice were obtained from the Jackson Laboratory. Stereotaxic injection of AAV was performed using the following coordinates: anterioposterior = −2 mm from Bregma, lateral = ±1.5 mm; ventral = 2.2 mm. For the cell survival assay, optical fibers (Doric Lenses) were implanted at the same injection sites following AAV injection at a depth of 1.6 mm from the skull surface. Mice were then allowed to recover for 4 weeks before analyses. The specificity and efficacy of expression of opsins in PV$^+$ and SST$^+$ neurons have been previously characterized[9]. All animal procedures were performed in accordance with institutional guidelines with approval from The Johns Hopkins University School of Medicine Animal Care and Use Committee.

***In vivo* optogenetic manipulation, immunostaining, confocal imaging, processing and quantification.** For analysis of neurogenesis after optogenetic and environmental manipulation[23], adult *Pvalb-cre* or *Sst-cre* mice at 4 weeks after AAV injection were pulsed with EdU (32.5 mM EdU stock solution, 41.1 mg per kg of body weight, intraperitoneal) four times with an interval of 2.5 h. 24 h after the first EdU injection, the *in vivo* light procedure was administered as previously described[9]. For ChR2 stimulation, blue light flashes (472 nm) lasting 5 ms at 8 Hz programmed by Master 8 through DPSSL laser system (Laser century) were delivered *in vivo* every 5 min for 30 s per trial. For eNpHR or Arch stimulation, continuous yellow light (593 nm) was delivered *in vivo*. For opsin stimulation, the whole light stimulation procedure lasted 8 h d^{-1} for 4 consecutive days (**Supplementary Figs. 6a** and **8a**). At the end of the fourth day, mice were processed for immunohistology. Given the expected light spread *in vivo*, every sixth section within a distance of 1.0 mm anterior and posterior to injection sites was used for quantification and analysis. Histological and electrophysiological analyses showed that these treatments did not lead to defects in the structural integrity of the dentate gyrus, substantial cell death or changes of PV$^+$ neuron properties in the adult dentate gyrus[9]. For immunohistology, coronal brain sections (40 μm in thickness) were processed as previously described[5]. EdU labeling was processed using Click-iT EdU Alexa Fluor imaging kit (Invitrogen). We used antibodies to Tbr2 (Abcam, rabbit, 1:1,000), DCX (Santa Cruz, goat, 1:500), MCM2 (BD, mouse, 1:500), PV (Swant, mouse, rabbit or goat, 1:5,00), SST (Millipore, rat, 1:200), synapsin I (Molecular Probes, rabbit, 1:500), GAD67 (Chemicon, mouse or rabbit, 1:500), Iba-1 (Millipore, rabbit, 1:500), NeuN (Millipore, mouse, 1:500) and NeuroD (Santa Cruz, goat, 1:250). Images were acquired on a Zeiss LSM 710 multiphoton confocal system (Carl Zeiss) using a multi-track configuration. Stereological quantification was assessed in the adult SGZ as previously described[27]. For dendritic analysis, three-dimensional reconstruction of entire dendritic processes of each newborn neuron at 10 dpi was made from *z* series stacks of confocal images. The two-dimensional projection images were traced with ImageJ (US National Institutes of Health). All newborn dentate granule neurons with largely intact dendritic trees were analyzed for total dendritic length as described[5,28]. The measurements did not include corrections for inclinations of dendritic process and therefore represented projected lengths. Sholl analysis for dendritic complexity was carried out by counting the number of dendrites that crossed a series of concentric circles at 10-μm intervals from the soma as previously described[28]. All quantifications were performed by investigators blind to experimental conditions.

Electron microscopy analyses. Adult *Pvalb-cre* mice were stereotaxically injected with DIO-GFP AAV, followed by injection of retroviruses expressing GFP 4 weeks later. 4 d after retroviral injection, mouse brains were processed for immunoelectron microscopy as previously described[29,30]. Briefly, mice were transcardially perfused with 4% paraformaldehyde (wt/vol) in 0.1 M phosphate-buffered saline (PBS), pH 7.4, and maintained at 4 °C. Brains were removed 15 h after the perfusion and post-fixed for 72 h in 4% paraformaldehyde in 0.1 M PBS. Coronal sections (50 μm thick) were then sectioned using a vibratome and observed with an epifluorescence microscope. Sections containing clearly labeled newborn progeny and PV$^+$ terminals were cryoprotected in 2% glycerol and 20% DMSO (vol/vol) in 0.1 M PBS for 20 min and freeze-thawed four times in liquid nitrogen. After a treatment in 0.3% hydrogen peroxide in 0.1 M PBS (vol/vol, five times for 5 min) and three 10-min washes in 0.5% bovine serum albumin in 0.1 M PBS (vol/vol, BSA-C, Aurion), sections were incubated overnight in the primary antibody (rabbit antibody to GFP, Invitrogene, 1:500; A11122) in 0.1% BSA-C in 0.1 M PBS, 40 h at 4 °C on a shaker). After washing in 0.1% BSA-C in 0.1 M PBS, the sections were incubated for 5 h at 20 ± 5 °C in biotinylated secondary antibody (goat antibody to rabbit, F_{ab} fragment, Jackson Laboratories, 1:200, 111 066 047, 0.1% BSA-C in 0.1 M PBS). Sections were incubated for 2 h in avidin biotin peroxidase complex (ABC Elite, Vector Laboratories), followed by a reaction with 3,3-diaminobenzidine (Vector Laboratories Kit, 10–20 min). The sections were then post-fixed overnight in 2.5% glutaraldehyde in 0.1 M phosphate buffer (vol/vol), washed in 0.1 M PBS, post-fixed in osmium tetroxide for 1 h, dehydrated in ascending concentrations of ethanol and then acetone, and embedded in Epoxy resin. Locations of clearly labeled newborn progeny and PV$^+$ terminals were identified at the light microscopic level (**Supplementary Fig. 4a**,**m**) and followed through to the electron microscopic level. Serial sections (60 nm thick) were collected on single-slot copper grids and contrasted by incubating for 35 min in 5% uranyl acetate solution in dH_2O (wt/vol) and then 25 min in a Reynolds solution. Sections were then examined using a Philips CM10 transmission electron microscope and serial images of the labeled structures were captured using a digital camera (Morada SIS, Olympus). These images were then aligned and three-dimensional structures were rendered using Fiji and 3D Studio Max software (**Fig. 1a**,**c** and **Supplementary Figs. 1c** and **4f**).

Electrophysiology analysis. Adult mice housed under standard conditions were processed at 3–7 dpi for slice preparation as previously described[5,9,22]. The brains were quickly removed into the ice-cold solution (110 mM choline chloride, 2.5 mM KCl, 1.3 mM KH_2PO_4, 25.0 mM $NaHCO_3$, 0.5 mM $CaCl_2$, 7 mM $MgSO_4$, 20 mM dextrose, 1.3 mM sodium L-ascorbate, 0.6 mM sodium pyruvate, 5.0 mM kynurenic acid). Slices (275 μm thick) were cut using a vibrotome (Leica VT1000S) and transferred to a chamber containing the external solution (125.0 mM NaCl, 2.5 mM KCl, 1.3 mM KH_2PO_4, 1.3 mM $MgSO_4$, 25.0 mM $NaHCO_3$, 2 or 5 mM $CaCl_2$, 1.3 mM sodium L-ascorbate, 0.6 mM sodium pyruvate, 10 mM dextrose, pH 7.4, 320 mOsm), bubbled with 95% O_2/5% CO_2. Electrophysiological recordings were obtained at 32–34 °C. GFP$^+$ or RFP$^+$ cells in the SGZ were visualized by differential interference contrast and fluorescence microscopy. Mature granule cells in the outer granule cell layer in the same slices were recorded for comparison. The whole-cell patch-clamp configuration was employed in the voltage-clamp mode (V_m = −65 mV). Microelectrodes (4–6 MΩ) were pulled from borosilicate glass capillaries and filled with the internal solution containing 135 mM CsCl gluconate, 15 mM KCl, 4 mM $MgCl_2$, 0.1 mM EGTA, 10.0 mM HEPES, 4 mM ATP (magnesium salt), 0.3 mM GTP (sodium salt), 7 mM phosphocreatine (pH 7.4, 300 mOsm). Additional chemicals were used at the following final concentrations in the bath as indicated: bicuculline (50–100 μM), CNQX (20 μM) and AP5 (50 μM). All chemicals were purchased from Sigma except bicuculline (Tocris). Data were collected using an Axon 200B amplifier and acquired with a DigiData 1322A (Axon Instruments) at 10 kHz. For measuring GABA-induced responses from GFP$^+$ cells, focal pressure ejection of 10 μM GABA through a puffer pipette controlled by a Picospritzer (5-ms puff at 3–5 psi) was used to activate $GABA_A$Rs. A bipolar electrode (World Precision Instruments) was used to stimulate (0.1-ms duration) the dentate granule cell layer. Low frequency (0.1 Hz) and theta bursts (5 Hz, 10-s duration) were delivered to stimulate the granule cell layer in the presence or absence of bicuculline (100 μM). The stimulus intensity (50 μA) was maintained for all experiments.

For experiments with light stimulation of PV$^+$ or SST$^+$ neurons, retroviruses expressing RFP were stereotaxically delivered to the adult dentate gyrus to label proliferating neural progenitors at 4 weeks after AAV injection. Electrophysiology recordings were performed 4 d after retroviral injection. To stimulate ChR2 in PV$^+$ or SST$^+$ neurons, light flashes (0.1 or 8 Hz) generated by a Lambda DG-4

plus high-speed optical switch with a 300-W Xenon lamp and a 472-nm filter set (Chroma) were delivered to coronal sections through a 40× objective (Carl Zeiss). To stimulate eNpHR or Arch in PV^+ neurons, continuous yellow light generated by DG-4 plus system with a 593-nm filter set was delivered to coronal sections through a 40× objective as previously described[9].

Statistical analysis. Detailed statistical information can be found in **Supplementary Table 1**. Statistical analysis was performed with one-way ANOVA (with Tukey *post hoc* test), two-tailed unpaired Student's *t* test or two-sample Kolmogorov-Smirnov test, as indicated in the text and figures. When a significant interaction was found upon performing two-way ANOVA, simple main effects were determined by a two-tailed unpaired Student's *t* test. Validation of normality and homogeneity of variance assumptions was performed for all compared data groups using Shapiro-Wilk and Levene's tests, respectively. All statistical analyses were performed using Origin software (OriginLab) or Matlab (MathWorks).

21. van Praag, H. *et al. Nature* **415**, 1030–1034 (2002).
22. Ge, S., Yang, C.H., Hsu, K.S., Ming, G.L. & Song, H. *Neuron* **54**, 559–566 (2007).
23. Kempermann, G., Kuhn, H.G. & Gage, F.H. *Nature* **386**, 493–495 (1997).
24. Atasoy, D., Aponte, Y., Su, H.H. & Sternson, S.M. *J. Neurosci.* **28**, 7025–7030 (2008).
25. Sohal, V.S., Zhang, F., Yizhar, O. & Deisseroth, K. *Nature* **459**, 698–702 (2009).
26. Cardin, J.A. *et al. Nature* **459**, 663–667 (2009).
27. Kim, J.Y. *et al. Neuron* **63**, 761–773 (2009).
28. Duan, X. *et al. Cell* **130**, 1146–1158 (2007).
29. Toni, N. *et al. Nat. Neurosci.* **11**, 901–907 (2008).
30. Toni, N. *et al. Nat. Neurosci.* **10**, 727–734 (2007).